Potential Role of FDG-PET Imaging in Understanding Tumor-Host Interaction

Robert A. Gatenby

Department of Diagnostic Imaging, Temple University Hospital, Philadelphia, Pennsylvania

Population ecology mathematical models of tumorigenesis have been developed to define the cellular characteristics which allow a transformed population to begin as a single individual but end with complete destruction of the host. To invade and expand, a tumor population must compete successfully with normal cells for space and critical, shared substrate such as glucose. This study uses population ecology models to examine the potential role of competition for glucose in tumor biology and its implications for FDG-PET imaging. **Methods:** Chemostat population ecology mathematical models of the tumor-host interface are developed resulting in coupled, nonlinear differential equations which link population growth to acquisition and utilization of glucose. **Results:** The models demonstrate that increased FDG uptake in tumors observed on PET imaging is the result of increased consumption necessary to provide surplus energy for reproduction when inefficient glycolytic pathways are used for glucose metabolism. Specific parameters of the glucose consumption curves are predicted to be markedly different in normal and neoplastic tissues and critical to the tumor-host interaction. Tumor invasability and patient prognosis can be linked to these parameters. **Conclusion:** The mathematical models link FDG-PET imaging with processes fundamental to the outcome of the tumor host interaction. The value of FDG-PET can be expanded by quantitation of glucose uptake parameters which will be highly specific in tumor detection and strong indicators of tumor aggressiveness. Therapeutic modalities designed to decrease tumor glucose uptake or increase glucose uptake in normal tissue could be directed and monitored by FDG-PET.

Key Words: emission computed tomography; neoplasm; tumor-host interaction; glucose; radionuclide imaging

J Nucl Med 1995; 36:893–899

PET with 2-[^{18}F]fluoro-2-deoxy-D-glucose (FDG) has demonstrated great clinical utility in imaging a variety of cancers including lung (*1,2*) head and neck (*3*), breast (*4*), bladder (*5*) and brain (*6,7*), as well as lymphomas (*8*) and colon cancer hepatic metastases (*9*). FDG is a glucose analog which is transported intracellularly and phosphorylated but not further metabolized (*10*). Its value in imaging relies on increased uptake and utilization of glucose by transformed cells when compared to normal cells, a trait first recognized by Warburg (*11*) over 60 yr ago. More recent investigations have determined that this increased uptake is the result of larger numbers of glucose transporter polypeptides on the cell surface which are linked to oncogene activation and is a very early phenotypic change following transformation (*12–14*). Increased glucose utilization is the result of increased levels of intracellular enzymes such as hexokinase and phosphofructokinase which promote glucose metabolism through the glycolytic pathway (*15*) despite its inefficiency in energy production (2 mole ATP per 1 mole of glucose verses 38 mole ATP produced via the TCA pathway (*16*)) and the resulting formation of lactate and H^+ ions.

Population ecology models provide a novel conceptual framework for investigating tumor-host interaction (*17,18*). In this paradigm, each volume of normal tissue is considered a cellular community populated by "species" of epithelial and mesenchymal cells in a dynamic equilibrium with each other and the environment. Malignant transformation produces one or a small number of individuals forming a new, tumor "species" which disturbs the ecological stability of this cellular community. For tumorigenesis, the transformed cells must evolve properties which allow acquisition of space and resources from the existing populations despite the numerical advantage of the latter and the inhibitory activities of the host response. Interaction of the tumor population with native host cells may result in three general outcomes: (1) extinction of the original population, resulting in invasive tumor growth; (2) a stable equilibrium in which the transformed cells co-exist with the normal cells, resulting in limited tumor growth such as a benign lesion or carcinoma in situ; and (3) extinction of the tumor population.

In nature, the outcome of competition between populations frequently depends on the efficiency with which each population utilizes a critical, shared resource (*19,20*). Because of its central role in energy production, glucose may be a critical, shared resource at the tumor-host interface. This work examines the potential advantage increased glucose uptake might confer on transformed populations and

Received Jun. 20, 1994; revision accepted Sept. 30, 1994.

For correspondence or reprints contact: Robert A. Gatenby, MD, Department of Diagnostic Imaging, Temple University Hospital, Broad and Ontario Streets, Philadelphia, PA 19140.

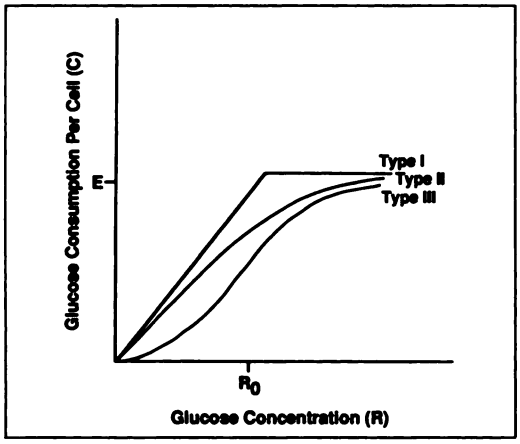

FIGURE 1. Possible curves of glucose consumption at varying concentrations as described by Holling. Types II and III approach saturation gradually while type I is abrupt. Type III is less efficient at low glucose levels. The saturation level E and half-saturation value R_0 for the Holling type III consumer is shown.

its implications for tumor biology and FDG-PET tumor imaging.

MATHEMATICAL MODEL

Glucose Assimilation and Utilization by Cellular Populations

Uptake and utilization of any resource (R) necessary for cell maintenance and reproduction can be described as follows:

$$c_i = m_i + p_i; \quad i = 1, 2, \ldots, K, \qquad \text{Eq. 1}$$

where c = consumed resource/individual cell/unit time; m = resource utilized for maintenance/cell/unit time; and p = resource available for reproduction/cell/unit time for K resources.

Consumption or uptake (c) of each resource will vary depending on the amount of the resource available (R) and the capacity of the cell to acquire it. Thus,

$$c = f(R). \qquad \text{Eq. 2}$$

Holling (*21*) distinguished three typical shapes for the consumption curve c = f(R) as shown in Figure 1. Available data on glucose uptake by an individual cell suggest that it is best approximated by the Holling type III sigmoid response curve (*22*). This will be utilized in the remainder of the analysis, although it can be shown that the specific shape of the consumption curve does not affect the conclusion.

For a homogeneous population of N tumor or normal cells, the total resource absorbed and utilized per unit time is:

$$N\bar{c} = N\bar{m} + N\bar{p}, \qquad \text{Eq. 3}$$

where $\bar{c}$ = average consumed resource/cell; $\bar{m}$ = average resource utilization for maintenance/cell; and $\bar{p}$ = average resource accumulation for reproduction/cell. If a transformed population is to expand (dN/dt > 0), resources must be available for reproduction and thus $p > 0$ and $\bar{c} - \bar{m} > 0$. That is, glucose consumption ($\bar{c}$) must exceed its requirement for maintenance if the cell population is to increase.

In the absence of competing populations, cell population kinetics can be described by the logistic equation linked to consumption and metabolism as follows:

$$\frac{dN}{dt} = gN\left(1 - \frac{N}{N_{max}}\right)\frac{1}{\gamma}(\bar{c} - \bar{m}), \qquad \text{Eq. 4}$$

where resource accumulation and distribution is assumed to occur on a much faster time scale than cellular division; N_{max} is the maximum number of cells that can occupy a given volume of tissue if resources are unlimited and is related to constraints such as cell volume and cell-cell inhibition; g is the intrinsic rate of population growth (i.e., doubling time) if resources are unlimited and are dependent on a variety of factors such as the tumor cell genotype level of growth factors present and the number of growth factor receptors present on the cell surface; and γ is a conversion factor (*23*) for the transformation of resources into new individuals. In the remainder of this analysis, g/γ will be expressed as a single constant β.

For a Holling type III functional response, the population equation can be restated as:

$$\frac{dN}{dt} = \beta N\left(1 - \frac{N}{N_{max}}\right)\left(-\bar{m} + \frac{ER^2}{R_0^2 + R^2}\right), \qquad \text{Eq. 5}$$

where E is the saturation level for glucose consumption (the maximum amount of glucose which can be transported into the cell if its concentration [R] is unlimited) and R_0 is the half-saturation concentration of glucose (i.e., the value of R at which glucose consumption $\bar{c}$ is 1/2 of E) (Fig. 2).

From Equation 4, it is clear that, for the early tumor population to grow when $N < N_{max}$, it must either minimize glucose utilization for maintenance ($\bar{m}$) or maximize absorption ($\bar{c}$) for the range of glucose concentrations found within the volume of tissue from which the transformed population emerges. Clearly, the preferential use of the inefficient glycolytic pathways in tumor cells increases glucose requirements for maintenance. A compensatory increase in absorption of glucose is therefore required if tumor cells are to have adequate energy for proliferation.

Glucose Delivery and Distribution

In the absence of consumers, the rate of change of a resource in any given volume of tissue can be expressed as:

$$\frac{dR}{dt} = r\left(1 - \frac{R}{K}\right), \qquad \text{Eq. 6}$$

where r = the rate of resource delivery and K = the carrying capacity of the environment for that resource. When R = K, dR/dt = 0 because the resource lost by diffusion or outflow in the vasculature equals the inflow. In tissue, both K and r are heavily dependent on blood flow.

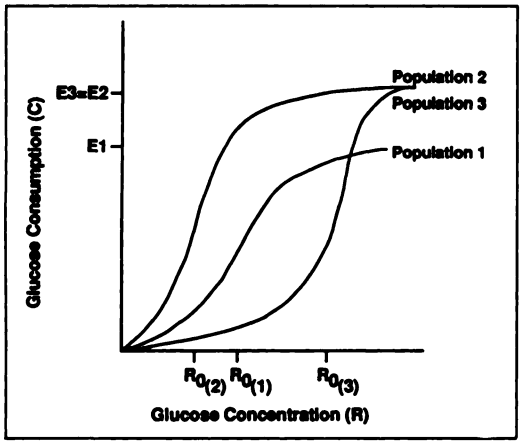

FIGURE 2. Three populations exhibiting different Holling type III consumption curves. Both E_3 and E_2 are larger than E_1 so that population 2 and 3 absorb more glucose at high concentrations. Because R_{01} is less than R_{03}, however, population 1 will absorb glucose more efficiently at lower concentrations. Because R_{02} is less than R_{03}, population 2 will absorb more glucose at low concentrations than population 3, even though the saturation value is the same for both.

A decrease in delivery because of slow blood flow or vascular destruction will diminish both parameter values. Figure 3 demonstrates two possible combinations or r and K in vascularized and nonvascularized tissue calculated from Equation 6.

When glucose consumption by a population of cells is considered, the resource kinetics can be expressed as:

$$\frac{dR}{dt} = r\left(1 - \frac{R}{K}\right) - N\bar{c}. \qquad \text{Eq. 7}$$

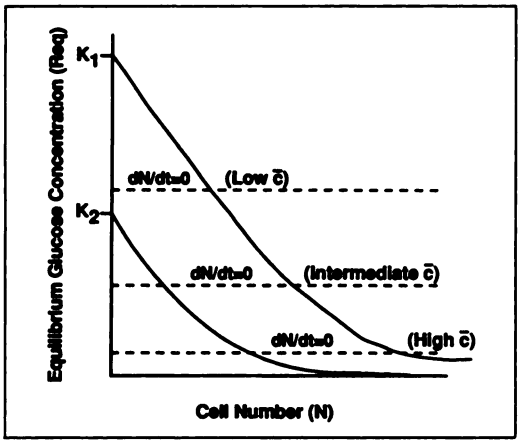

FIGURE 4. Solid lines represent the equilibrium states (dR/dt = 0) for any value of N for vascularized (K_1) and nonvascularized (K_2) tissue which are redrawn from computer-generated solutions of Equation 11. Dashed horizontal lines are equilibrium states dN/dt = 0 expressed in terms of R from Equation 10 for consumers of high, low, and intermediate efficiency of absorption (c). Note the change in the equilibrium value of N in vascularized and nonvascularized tissue demonstrated by the intersection of a dashed line with the two different solid curves.

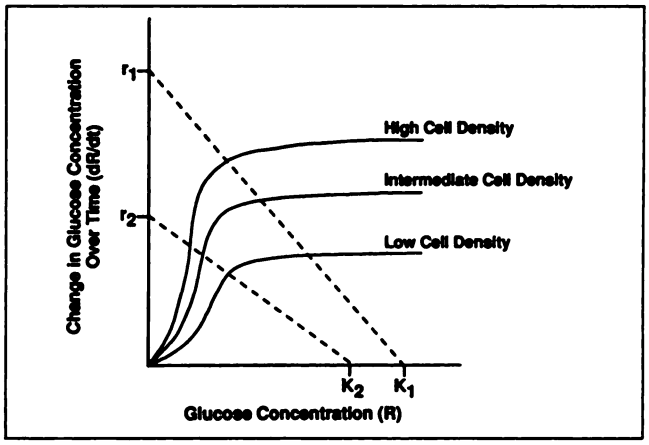

FIGURE 3. Dashed lines represent glucose delivery in the absence of consumers in vascular (K_1) and nonvascular (K_2) tissue. Solid lines are consumption curves for different densities of the same population N. The intersection of the solid and dashed lines represent equilibrium states (dR/dt = 0).

For the Holling type III consumption response this becomes:

$$\frac{dR}{dt} = r\left(1 - \frac{R}{K}\right) - N\left(\frac{ER^2}{R_0^2 + R^2}\right). \qquad \text{Eq. 8}$$

This is illustrated in Figure 3 which demonstrates the loss of glucose because of the presence of varying densities of a cellular population. For any level of R and N, dR/dt will be the result of subtracting the solid line from the dashed line. Equilibrium is achieved when dR/dt = 0 which is graphically represented by the intersection of a solid and dashed line.

Equilibrium of the cell population is achieved when dN/dt = 0. From Equation 5, it can be seen that if there is no limitation on glucose availability, dN/dt = 0 when N = N_{max}. If, however, the population is resource-limited and $N_{eq} < N_{max}$, then dN/dt = 0 when

$$\bar{m} = \frac{ER^2}{R_0^2 + R^2}, \qquad \text{Eq. 9}$$

which yields

$$R_{eq} = R_0\left(\frac{\bar{m}}{E - \bar{m}}\right)^{1/2},$$

where R_{eq} = the value of R at equilibrium.

Derivation of the equilibrium values of R and N are shown in Figure 4. The solid lines are the equilibrium value of glucose concentration (R) for any given N depending on the presence or absence of tumor vasculature and are derived from Equation 8 for dR/dt = 0 so that

$$N = \frac{r}{E}\left(1 + \left[\frac{R_0^2}{R^2} - \frac{R_0^2}{RK} - \frac{R}{K}\right]\right). \qquad \text{Eq. 10}$$

The equilibrium value of glucose concentration (R_{eq} when dN/dt = 0 from Equations 5 and 9) for a resource-limited

population with three levels of consumption are shown by the dashed lines. The entire system is in equilibrium when $dN/dt = dR/dt = 0$ and is shown as the intersection of the dashed lines with the solid lines.

If tumor expansion into a volume of tissue results in destruction of the vasculature in that volume, K_1 and r_1 in Equation 7 will be replaced by K_2 and r_2. Since $K_2 < K_1$ and $r_2 < r_1$, dR/dt will initially be <0 (because $R/K_1 < R/K_2$), thus reducing resources within the tissue and resulting in $dN/dt < 0$ (from Equation 5). A new equilibrium will then be achieved with R returning to the initial R_{eq}, but with a new lower value of N (from Equation 10 and graphically demonstrated in Fig. 4), resulting in the death of some fraction of the original tumor cell population. This would cause areas to have paradoxically diminished FDG uptake on PET imaging (compared to surrounding tumor and normal tissues) such as that described in some brain metastases (*24*).

Thus, the interaction of the tumor cell population with the host environment can result in multiple possible equilibrium states with final cell density, glucose concentration and glucose utilization, depending on the carrying capacity of the environment (blood flow) and the capacity of the tumor cells to absorb and use the delivered glucose.

Cellular Competition at the Tumor-Host Interface

Thus far, growth of transformed populations has been analyzed in the absence of other cells. In most situations, however, the tumor species expands into an ecological environment completely filled by existing species of normal cells in equilibrium with each other and the available resources. Thus, individual tumor cells at this interface must compete successfully with normal cells for these resources if they are to invade this volume of tissue.

Consider two species (Fig. 5) competing for a limited resource (glucose) with a Holling type III functional response. One population (N_1) consists of tumor cells, while the other consists of the host cells normally present (N_2). In this analysis, the heterogeneity of tumor cell societies and the varied cell types present in normal tissue are simplified by averaging the various subpopulations. A more realistic approach would expand the number of competing populations into several tumor subpopulations (N_{1a}, N_{1b}, N_{1c}, etc.) and normal cell populations (N_{2a}, N_{2b}, N_{2c}, etc.). This, however, markedly increases the complexity of the mathematical analysis without altering the general conclusions and will not be pursued further at this time.

The small volume of tissue in which the tumor cells and normal cells meet (i.e., the tumor edge) can be analyzed using Lotka-Volterra equations modified to take substrate absorption into account, resulting in the following coupled, nonlinear differential equations describing population and resource kinetics:

$$\frac{dN_1}{dt} = \beta_1 N_1\left(1 - \frac{N_1}{N_{1_{max}}} - \frac{\lambda_{12}N_2}{N_{1_{max}}}\right)\left(-\overline{m_1} + \frac{E_1R^2}{R_{01}^2 + R^2}\right), \quad \text{Eq. 11}$$

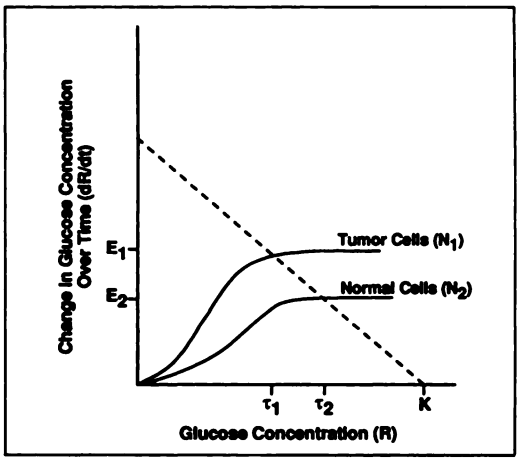

FIGURE 5. The dashed line represents the rate of increase in glucose concentrations (dR/dt) at different glucose levels (R) within a volume of tissue when no consumers are present. The tissue is at equilibrium when R = K. The solid curves represent two Holling type III populations. The tumor cells (population 1) have a larger E and a smaller R_0 than the normal cells. The intersection of the glucose deliver line with the consumption curve of each population represents the equilibrium state for that population. Clearly the tumor population achieves equilibrium at a lower concentration of glucose (τ_1) than the normal population.

$$\frac{dN_2}{dt} = \beta_2 N_2\left(1 - \frac{N_2}{N_{2_{max}}} - \frac{\lambda_{21}N_1}{N_{2_{max}}}\right)\left(-\overline{m_2} + \frac{E_2R^2}{R_{02}^2 + R^2}\right), \quad \text{Eq. 12}$$

$$\frac{dR}{dt} = r\left(1 - \frac{R}{K}\right) - N_1\left(\frac{E_1R^2}{R_{01}^2 + R^2}\right) - N_2\left(\frac{E_2R^2}{R_{02}^2 + R^2}\right), \quad \text{Eq. 13}$$

where $\lambda_{12}N_2$ is the interactive term measuring the effect of population N_2 on N_1 (a combination of negative effects such as cell-cell contact inhibition and immunologic attack and positive effects such as paracrine and endocrine growth factors) and λ_{12} is the competition coefficient; $\lambda_{21}N_1$ is the interactive term coefficient measuring the effect of the tumor population on the normal cells (i.e., production of growth factors or substances such as lactic acid which are toxic to normal cells) and λ_2, is the competition coefficient.

No empiric solution exists for these equations. Analysis at the boundaries, however, can provide significant insight. First, consider a volume of normal tissue in which the transformed population is just beginning its invasion so that $N_1 << N_{1max}$. This would correspond to a tumor edge. Tumor growth will occur only if $dN_1/dt > 0$. Inspection of Equation 11 demonstrates that $dN_1/dt > 0$ if:

$$1 - \frac{N_1}{N_{1_{max}}} - \frac{\lambda_{12}N_2}{N_{1_{max}}} > 0, \quad \text{Eq. 14}$$

and

$$-\overline{m_1} + \frac{E_1R^2}{R_{01}^2 + R^2} > 0. \quad \text{Eq. 15}$$

For N_1, small N_1/N_{1max} can be approximated as 0 and Equation 14 becomes

$$\lambda_{12} < \frac{N_{1_{max}}}{N_2}. \qquad \text{Eq. 16}$$

The author has discussed this condition in considerable detail elsewhere (*18*). It essentially quantifies the minimum host immune response required to prevent tumor growth. It can be shown (*18*) that this term is dominant very early following transformation when the tumor population is small. Its importance diminishes once the tumor population is established and will not be further discussed here. In the remainder of this study, however, it is important to keep in mind that while adequate substrate for reproduction is a necessary condition for tumor growth, other growth constraints may exist.

Equation 15 defines the additional constraint that resource uptake exceed maintenance needs and will be the focus of this analysis using a technique similar to that employed by Armstrong and McGehee (*25*).

Prior to transformation and the emergence of a tumor clone, normal cells will have achieved an equilibrium in which

$dN_2/dt = dR/dt = 0$ at some values $N_2 = \Delta_2$ and $R_2 = \tau_2$,

where $\Delta_2 = N_{2max}$ or, if the population is resource limited (probably a highly unusual phenomenon in normal tissue), Δ_2 is the population at which

$$-\overline{m_2} + \frac{E_2(\tau_2)^2}{R_{02}^2 + (\tau_2)^2} = 0, \qquad \text{Eq. 17}$$

and

$$r\left(1 - \frac{\tau_2}{K}\right) - \frac{E(\tau_2)^2}{R_{01}^2 + (\tau_2)^2} = 0. \qquad \text{Eq. 18}$$

If a small number of tumor cells ($N_1 \ll N_{1max}$) enters or arises in this volume of normal tissue, the tumor population will grow if $dN_1/dt > 0$ and thus

$$-\overline{m_1} + \frac{E_1(\tau_2)^2}{R_{01}^2 + (\tau_2)^2} > 0. \qquad \text{Eq. 19}$$

If $dN_1/dt > 0$, then N_1 will continue to increase until a new steady state is reached ($dN_1/dt = 0$) at equilibrium values of $N_1 = \Delta_1$, and $R = \tau_1$.

This represents the tumor's invasability and it is clear from the above analysis that the tumor population (N_1) can invade the normal cell population if $\tau_2 > \tau_1$. As shown in Figure 5, τ_1 will be less than τ_2 if the population N_1 is more efficient at glucose absorption in the range of glucose concentration (R) found within tissue. The invasability of the normal cells into the tumor cells can be analyzed similarly. If tumor cells are at equilibrium at $R = \tau_1$, then

$$\overline{m_2} + \frac{E_2(\tau_1)^2}{R_{02}^2 + (\tau_1)^2} < 0. \qquad \text{Eq. 20}$$

Thus, interstitial glucose concentrations at the tumor-host interface should decrease significantly because of enhanced tumor consumption. The resulting substrate deficiency prevents normal cells from dominating or even coexisting with the tumor cells. The invasability and, therefore, malignancy of a population can be critically linked to its ability to gather glucose more efficiently than the normal population with which it competes.

Implications for FDG-PET Imaging

For the tumor population to have adequate energy for reproduction, Equations 17 and 18 can be combined to show that for the substrate source of that energy the following relationship must hold:

$$R_{01}\left(\frac{\overline{m_1}}{E_1 - \overline{m_1}}\right)^{1/2} < R_{02}\left(\frac{\overline{m_2}}{E_2 - \overline{m_2}}\right)^{1/2}. \qquad \text{Eq. 21}$$

Data from FDG-PET imaging of lung and head and neck cancers have shown glucose uptake (c) to be increased in tumors generally six- to eight-fold (*1–6*) when compared to normal tissue. In vitro studies (*11,14,15*), however, show preferential use of the inefficient glycolytic pathway in tumors and indicate that $\bar{m}_1$ is significantly greater than $\bar{m}_2$. For example, a change from 0% to 100% glycolysis would increase glucose needs for maintenance ($\bar{m}$) by a factor of 19 (*16*). Thus, a change to glycolysis without compensatory mechanisms will actually *decrease* the probability of tumor growth by increasing the $(\bar{m}_1/E_1 - \bar{m}_1)^{1/2}$ term. It is thus clear that tumor growth is strongly dependent on minimization of R_{01} and maximization of E_1. This would correspond to a Holling type III consumption curve for tumor with a steep, early upslope (small R_{01}) and high plateau (large E_1) when compared to normal cells. The resulting increased consumption which is seen in FDG-PET imaging will also dramatically reduce R_{eq} in the interstitium at the tumor-host interface (from Equation 9). The reduction of glucose availability to normal cells reduces viability when glucose uptake (c) declines below maintenance needs (m), thus facilitating tumor invasion.

Therefore, increased tumor glucose uptake which allows FDG-PET imaging is also a fundamental process in the tumor-host interaction. The models predict that in addition to increased tumor uptake, FDG-PET should image decreased uptake in adjacent normal tissue (although this effect may exist over a range of only two to three cell layers and thus may not be observable with current PET technology). Finally, quantitation of R_{01}, and E_1 from pre-equilibrium FDG-PET images will provide more sensitive and specific criteria for tumor detection. Furthermore, Equation 21 shows that the difference between τ_1 and τ_2 will be a powerful predictor of tumor aggressiveness, thus linking the differences between E_1, and E_2, and R_{01} and R_{02} with patient prognosis.

DISCUSSION

Tumorigenesis is the result of multiple genetic changes each one insufficient in itself to produce a transformed

phenotype, but when summed by accumulation, result in cancer (*26,27*). Although oncogenesis must be understood at a molecular level, it is imperative to also understand how these genotypic changes and their resulting phenotypic expression act at a cellular level, conferring on a tumor population advantages which allow it to start as a single cell and end with complete destruction of the host.

Although population ecology models require oversimplification of this complex biological process, they do provide useful insights into the basic mechanisms which are functioning at a cellular level. The models predict that a major factor in the tumor-host interaction could involve competition for a critical, shared resource. They suggest, therefore, that the markedly increased glucose uptake by transformed cells measured in vitro and confirmed in vivo by FDG-PET may confer significant advantages on the tumor cells. First, it provides the tumor cells with adequate substrate for unconstrained proliferation. Second, it diminishes glucose concentrations available to adjacent normal cells. The consequent reduction in energy production will reduce the viability of the normal tissue facilitating tumor invasion. Finally, the lactate and acid production will reduce interstitial pH which may also reduce viability of normal cells.

This theoretical analysis is supported by experiments at a cellular and molecular level. Flier et al. (*13*) demonstrated that increased glucose transport is induced by the ras and src oncogenes. Growth factors have been shown to induce increased expression of the glucose transporter gene by Hiraki et al. (*28*). Birnbaum et al. (*12*) demonstrated increased transcription of glucose transporter gene occurred very rapidly following transformation of fibroblasts. Weber (*29*) correlated the rate of tumor growth with the magnitude of increased glycolysis.

FDG-PET has demonstrated considerable success in imaging tumors and is clearly valuable in both detecting and staging cancer (*1–6*). This technique is also able to quantify glucose uptake by tissues and several studies have correlated this quantitative information with tumor aggressiveness and patient prognosis. Patz et al. (*30*) were able to distinguish benign from malignant pulmonary nodules because of increased glucose uptake in malignant lesions. Di Chiro (*31*) found that the glucose metabolic rate of malignant gliomas correlated linearly with their histologic grade. Di Chiro et al. (*32*) correlated increased FDG uptake with increased aggressivity and probability of recurrence in intracranial meningiomas. Alavi (*33*), Kim (*34*) and Patronas et al. (*35*) have demonstrated correlation of glucose uptake with prognosis in patients with brain tumors. Haberkorn et al. (*36*) found increased relative glucose uptake in cancers of the head and neck associated with increased proliferative activity (percentage of cells in the S- and G2/M phases of the cell cycle). Adler et al. (*37,38*) found correlation of FDG uptake with the histologic grade of liposarcomas and other soft-tissue sarcomas. Okada et al. (*39*) correlated glucose uptake with prognosis in lymphoma. Francavilla et al. (*40*) were able to use foci of increased FDG uptake to malignant degeneration in low grade gliomas. Haberkorn et al. (*41*) correlated glucose uptake with patient response to radiotherapy and Ichiya et al. (*42*) demonstrated variable decreased uptake in a variety of tumors using different therapeutic regimens.

A significant prediction of the mathematical models is that increased tumor substrate uptake will diminish the availability and therefore the metabolism in surrounding normal tissue. Although it is likely that this effect generally acts within a distance too small to be observed with current PET technology, one group has reported diminished metabolism in normal brain parenchyma surrounding tumor (*43*).

CONCLUSION

Population ecology analysis concludes that FDG-PET is imaging a phenomenon fundamental to the outcome of the tumor-host interaction and provides a theoretical basis for the observed correlation of tumor aggressiveness and patient prognosis with quantitation of glucose uptake. The model also predicts that measurement of E and R_0 in tumor and adjacent normal tissues will enhance the value of FDG-PET in tumor detection and in estimating patient prognosis. It predicts that cells adjacent to tumor should be glucose-deprived because of a tumor-induced decrease in interstitial concentrations, an effect which should be observable when sufficient resolution has been achieved and which should also have prognostic significance. Finally, the models predict that new therapeutic modalities can be developed which either decreased glucose uptake in tumors or increased uptake by normal cells adjacent to the tumor. FDG-PET will be necessary to direct and monitor these therapeutic interventions.

ACKNOWLEDGMENTS

The author thanks Milena Herman for her skill and patience and Drs. Robert Stern, David Charkes, Barton Milestone and William King for their helpful suggestions.

REFERENCES

1. Patz EF Jr, Lowe VJ, Hoffman JM, Paine SS, Harris LK, Goodman PC. Persistent or recurrent bronchogenic carcinoma: detection with PET and 2-[F-18]-2-deoxy-D-glucose. *Radiology* 1994;191:379–382.
2. Wahl RL, Quint LE, Greenough RL, Meyers CR, White RI, Orringer MB. Staging of mediastinal non-small cell lung cancer with FDG PET, CT and fusion images: preliminary prospective evaluation. *Radiology* 1994;191:371–377.
3. Jabour BA, Choi Y, Hoh CK, et al. Extracranial head and neck: PET imaging with 2-[F-18]fluoro-2-deoxy-D-glucose and MR imaging correlation. *Radiology* 1993;186:27–35.
4. Wahl RL, Cody RL, Hutchins GD, Mudgett EE. Primary and metastatic breast carcinoma: initial clinical evaluation with PET with the radiolabeled glucose analogue 2-[F-18]-fluoro-2-deoxy-D-glucose. *Radiology* 1991;179: 765–770.
5. Harney JV, Wahl RL, Liebert M, et al. Uptake of 2-deoxy, 2-(^{18}F)fluoro-D-glucose in bladder cancer: animal localization and initial patient positron emission tomography. *J Urol* 1991;145:279–283.
6. Di Chiro G. Positron emission tomography using [^{18}F]fluorodeoxyglucose in brain tumors. *Invest Radiol* 1981;22:360–371.
7. Di Chiro G, Brooks RA. PET-FDG of untreated cerebral gliomas. *J Nucl Med* 1988;29:421–422.
8. Paul R. Comparison of fluorine-18-2-fluorodeoxyglucose and gallium-67-

citrate imaging for the detection of lymphoma. *J Nucl Med* 1987;28:288–292.
9. Yonekura Y, Benua RS, Brill AB, et al. Increased accumulation of 2-deoxy-2[^{18}F] fluoro-D-glucose in liver metastasis from colon carcinoma. *J Nucl Med* 1982;23:1133–1137.
10. Gallagher BM, Fowler JS, Gutterson NT, et al. Metabolic trapping as a principle of radiopharmaceutical design: some factors responsible for the biodistribution of [^{18}F]2-Deoxyglucose. *J Nucl Med* 1978;19:1154–1161.
11. Warburg O. *The metabolism of tumors* (translated in English by F. Dickens). London: Constable; 1930:5–47.
12. Birnbaum MJ, Haspel HC, Rosen OM. Transformation of rat fibroblasts by FSV rapidly increases glucose transporter gene transcription. *Science* 1987; 235:1495–1498.
13. Flier JS, Mueckler MM, Usher P, et al. Elevated levels of glucose transport and transporter messenger RnA are induced by ras and src oncogenes. *Science* 1987;235:1492–1495.
14. Hoffman FA. Metabolic changes in malignancy. In: Liotta LA, ed. *Cancer growth and progression*. Boston: Kluwer Academic Publishers; 1989:18–27.
15. Monakhov NK, Neistadt EL, Shavlovskli MM, Shvartsman AL, Neifakh SA. Physicochemical properties and isoenzyme composition of hexokinase from normal and malignant human tissues. *J Natl Cancer Inst* 1978;61:27–34.
16. Harris RA. Carbohydrate metabolism: major metabolic pathways and their control. In: Devlin T, ed. *Textbook of biochemistry with clinical correlations*. New York: Wiley-Liss, Inc.; 1993:292–300.
17. Gatenby RA. Population ecology issues in tumor growth. *Cancer Research* 1991;51:2542–2547.
18. Gatenby RA. Mathematical prediction of sequential genetic changes necessary for tumor growth: implications for tumor biology and treatment. *J Theoretical Biol* 1994: in press.
19. Tilman D. *Resource competition and community structure*. Princeton: Princeton University Press; 1982:43–61.
20. Lomnicki A. *Population ecology of individuals*. Princeton: Princeton University Press; 1988:20–42.
21. Holling CS. The components of predation as revealed by a study of small mammal predation of the European Pine Sawfly. *Can Entomol* 1959;91:293–320.
22. Hatanaka M. Transport of sugars in tumor cell membranes. *Biochem Biophys Acta* 1974;355:77–104.
23. MacArthur RH. *Geographical ecology*. New York: Harper and Row; 1972: 102–141.
24. Griffeth LK, Rich KM, Dehdashti F, et al. Brain metastases from non-central nervous system tumors: evaluation with PET. *Radiology* 1993;186: 37–44.
25. Armstrong RA, McGehee R. Competitive exclusion. *Am Naturalist* 1980; 115:151–170.
26. Cho KR, Vogelstein B. Genetic alterations in the adenoma-carcinoma sequence. *Cancer* 1992;70:1727–1731.
27. Weinberg RA. Oncogenes, antioncogenes and the molecular basis of multistep carcinogenesis. *Cancer Res* 1989;49:3713–3721.
28. Hiraki Y, Rosen OM, Birnbaum MJ. Growth factors rapidly induce expression of the glucose transporter gene. *J Biol Chem* 198;27:13655–13662.
29. Weber G. Enzymology of cancer cells. *N Engl J Med* 1977;296:486–493, 541–551.
30. Patz EF Jr, Lowe VJ, Hoffman JM, et al. Focal pulmonary abnormalities: evaluation with F-18 fluorodeoxyglucose PET scanning. *Radiology* 1993; 188:487–490.
31. Di Chiro G. Positron emission tomography using [^{18}F]fluorodeoxyglucose in brain tumors. A powerful diagnostic and prognostic tool. *Invest Radiol* 1987;22:360–371.
32. Di Chiro G, Hatazawa J, Katz DA, et al. Glucose utilization by intracranial meningiomas as an index of tumor aggressivity and probability of recurrence: a PET study. *Radiology* 1987;164:521–526.
33. Alavi JB, Alavi A, Chawluk J, et al. Positron emission tomography in patients with glioma: a predictor of prognosis. *Cancer* 1988;62:1074–1078.
34. Kim CK, Alavi JB, Alavi A, Renich M. New grading system of cerebral gliomas using positron emission tomography with F-18 fluorodeoxyglucose. *J Neuroncol* 1991;10:85–91.
35. Patronas NJ, Di Chiro G, Kufta C, et al. Prediction of survival in glioma patients by means of positron emission tomography. *J Neurosurg* 1985;62: 816–822.
36. Haberkorn U, Strauss LG, Reisser C, et al. Glucose uptake, perfusion and cell proliferation in head and neck tumors: relation of positron emission tomography to flow cytometry. *J Nucl Med* 1991;32:1548–1555.
37. Adler LP, Blair HF, Makley JT, et al. Noninvasive grading of musculoskeletal tumors using PET. *J Nucl Med* 1991;32:1508–1512.
38. Adler LP, Blair HF, Williams RP, et al. Grading liposarcomas with PET using [^{18}F]FDG. *J Comput Assist Tomogr* 1988;14:960–962.
39. Okada J, Toshikawa K, Imazeki K, et al. The use of FDG-PET in the detection and management of malignant lymphoma: a correlation of uptake with prognosis. *J Nucl Med* 1991;32:686–691.
40. Francavilla TL, Miletich RS, Di Chiro G, et al. Positron emission tomography in the detection of malignant degeneration of low grade gliomas. *Neurosurgery* 1989;24:1–5.
41. Haberkorn U, Strauss LG, Dimitrikopoulou A, et al. PET studies of fluorodeoxyglucose metabolism in patients with recurrent colorectal tumors receiving radiotherapy. *J Nucl Med* 1991;32:1485–1490.
42. Ichiya Y, Kuwabara Y, Otsuka M, et al. Assessment of response to cancer therapy using fluorine-18-fluorodeoxyglucose and positron emission tomography. *J Nucl Med* 1991;32:1655–1660.
43. Powe JE, Alavi JB, Hackney D, Reivich M. Cerebral metabolic changes in patients with brain tumors demonstrated by positron emission tomography. *J Neurol Imag* 1992;2:1–7.